Catalysis Letters (2018) 148:1951–1964
https://doi.org/10.1007/s10562-018-2405-5

Fast Cycling NOx Storage and Reduction: Identification of an Adsorbed Intermediate Pathway

Allen Wei-Lun Ting[1] · Michael P. Harold[1] · Vemuri Balakotaiah[1]

Received: 18 February 2018 / Accepted: 2 May 2018 / Published online: 14 May 2018

Abstract

An experimental study describes fast cycling NOx storage and reduction on a Pt/Rh/BaO/CeO_2/Al_2O_3 monolith catalyst for emission control of lean burn vehicles. Comparison of the temporal dependence of the effluent composition when using H_2 and C_3H_6 as reductants enables an assessment of the mechanism. Involvement of a surface N-containing oxygenate pathway is indicated by the appearance of peaks of N_2O, N_2, and CO_2 during the rich to lean switch. Adsorbed intermediate reactivity measurements provide further evidence.

Graphical Abstract

m/e = 28 signal indicating thermal decomposition and oxidation of HC-intermediates under lean/rich/blank cycle of different durations.

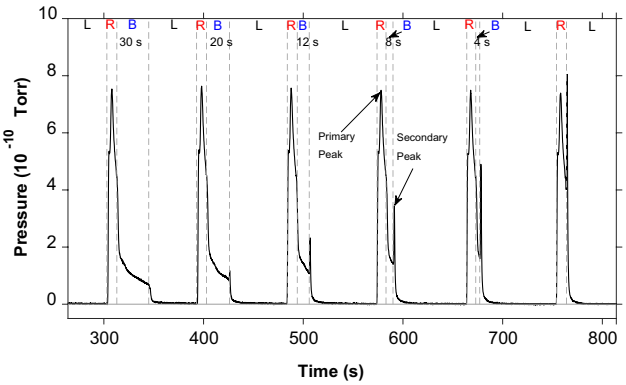

Keywords Propylene · NOx reduction · NOx storage · Platinum · Ceria

1 Introduction

As a result of more stringent regulations for NMOG + NOx (non-methane organic gases and nitrogen oxides, respectively) emissions, research on advancing NOx reduction efficiency in mobile exhaust has been active. Lean combustion engines such as those fueled by diesel have higher fuel efficiency than stoichiometric gasoline engines. However, the reduction of NOx in the lean exhaust is a challenge. NOx storage and reduction (NSR) is an innovative method that does not require the use of ammonia-generating urea as far as the selective catalytic reduction (SCR) method.

Electronic supplementary material The online version of this article (https://doi.org/10.1007/s10562-018-2405-5) contains supplementary material, which is available to authorized users.

✉ Michael P. Harold
mharold@uh.edu

[1] Department of Chemical & Biomolecular Engineering, University of Houston, Houston, TX 77204, USA

NSR is operated by cycling between two exhaust feeds to the lean NOx trap (LNT) catalyst, wherein NOx is stored during the lean phase of the cycle and reduced during the rich phase. One way to achieve the lean-rich switching is through direct fuel injection into the exhaust. During the lean feed, NOx is stored as nitrates and nitrites on BaO/$BaCO_3$ via NO oxidation to NO_2. Upon the switch to a rich feed, the stored NOx species are reduced to the preferred product N_2, and to undesired byproducts N_2O and NH_3. Due to the inherent kinetic, thermodynamic and mass-transport limitations along with exothermic heat effects, NSR has a narrow temperature range of high NOx conversion (~ 275 to 375 °C) [1, 2].

In order to keep pace with forthcoming emission rules, improvements in NSR technology have been proposed and investigated. The combination of coupled LNT and SCR with sequential or dual-layer configurations involves in-situ NOx reduction to NH_3 with its subsequent storage and reaction with unconverted NOx [3]. More recently, passive NOx adsorption (PNA) using Pd-exchanged zeolites has emerged as a method for trapping NOx at lower temperature encountered during the warmup phase or periods of low engine load [4]. The trapped NOx is released as the exhaust heats up, resulting in NOx release and reduction in a downstream SCR unit. A third technology involves fast cycling NSR, proposed by Toyota researchers, who coined the technology "Di-Air" (diesel NOx aftertreatment by adsorbed intermediate reductants) [5]. Through injection of hydrocarbons (such as the fuel) at a frequency as high as 2.5 Hz, NOx conversion can be enhanced, especially at temperatures exceeding 400 °C. An adsorbed HC-intermediate pathway is suggested to be responsible for the enhancement. Surface intermediates formed by reaction between NOx and HC and having sufficient thermal stability enable NOx reduction through their oxidation or decomposition during the lean phase of the cycle [6, 7]. Another path is NO decomposition over oxygen defects of ceria catalyst at temperature as high as 560 °C, a new perspective of the Di-Air system [8]. The current study examines mechanistic aspects of fast cycling NSR, motivated by the impressive performance of Di-Air.

The impact of fast cycling on NSR performance has been examined recently using the model reductant H_2 [9]. That study showed that a better utilization of stored NOx is enabled under fast cycling and results in significant NOx conversion enhancement over a wide temperature range (200–500 °C). A key to that study was the use of H_2 (without CO_2 in the feed) as it eliminated complications incurred through the use of HC or even CO. Based on earlier studies of conventional NSR, it is well known that the reductant identity affects LNT performance. Under slower lean-rich cycling H_2 is the most effective reductant, followed by CO and then HCs. In contrast, under fast lean-rich cycling, certain HCs emerge as the most effective reductant [10] with olefins typically more effective than alkanes. In another study, propylene showed a NOx conversion enhancement comparable to H_2 during fast cycling [11, 12], while propane was much less effective [13]. These findings suggested that NOx conversion enhancement obtained during fast cycling may result from a surface intermediate mechanism in addition to the aforementioned stored NOx utilization mechanism. Fisher and coworkers reported that the optimized cycle time is ~ 1 s using ethylene, which represents a balance between better NOx storage efficiency and consumption of reductants due to mixing [14, 15]. Finally, our recent work suggests that the hydrocarbon intermediate mechanism may not be as important as the effect of better utilization of NOx storage sites in enhancing NOx conversion under fast cycling [16]. Despite its relative significance, it is important to demonstrate its existence and further estimate its contribution to NOx reduction.

The reaction between NOx and model hydrocarbons such as propylene has been studied since 1970s using a variety of catalysts. Findings from these studies provide insight about potential new pathways other than the conventional one during fast cycling NSR. Burch et al. [17] reviewed the formation of organo-nitrogen species through the reaction between acetate species or other adsorbed oxidized hydrocarbon species with surface nitrates. The reduced species of nitrogen are readily formed through organo-nitrogen species, and form N_2 through N atom coupling. Other studies report similar reactions [18–21]. Based on these and other studies, the formation of the HC-intermediates from reaction between C_3H_6 and NO and their reactivity to reduce NO are possible. Surface intermediates with isocyanate, nitrile and other functional groups are detectable with DRIFTS, but their reactivity with NOx under net lean conditions, which determines its ability to enhance NOx conversion, is still unknown.

Earlier studies of NSR have suggested NOx reduction pathways different than the conventional storage and reduction pathway. Double peaks of N_2O, N_2 and CO_2 have been detected as the evidence of the surface intermediates. Breen et al. [22] reported double peaks of N_2 and N_2O when using H_2 and/or CO as the reductants at 250 and 350 °C in the presence of 10% H_2O and CO_2. The primary peak emerging right after the switch from lean to rich purportedly results from the reduction of stored NOx. The secondary N_2 peak occurs on the switch from rich to lean is proposed to result from the oxidation of a surface isocyanate while the one of N_2O is mainly from the reaction between stored NH_3 and stored NOx. Chansai et al. [23] studied the effect of CO_2 on the secondary N_2 peak when using H_2 as the reductant at 350 °C, showing that secondary N_2 peak requires the presence of CO_2 when using H_2, while no gas feed NH_3 is detected. Isocyanate species were detected using in-situ DRIFTS analysis during the rich period; this further relates

the second N_2 peak to the CO forming from the reverse water gas-shift (WGS) reaction. Dasari et al. [24] observed the secondary peak of N_2O and CO_2, proposing a possible isocyanate involved NOx reduction mechanism, and the hydrolysis of isocyanate forming NH_3 in the presence of H_2O. Bartova et al. [25] detected the second peaks of N_2, N_2O and CO_2 at 150 and 200 °C using H_2 and CO as the reductants. The secondary peak of N_2O may result from incomplete regeneration, like the reduction of stored NOx by isocyanate and NO dissociation at partially-oxidized precious metal (Pt, Pd, and Rh). Mracek et al. [26] used C_3H_6 as the reductant without the presence of CO_2 at 200 to 300 °C, showing that C_3H_6 generates a secondary N_2O peak at higher temperature.

The current study integrates these results and expands to a wider temperature range. The objective is to study the reaction pathway involving surface HC-intermediates and NOx under fast cycling conditions. This is accomplished by comparing the NOx reduction performance between using different reductants, H_2 and C_3H_6, the former which only follows the conventional mechanism in the absence of CO_2, and the latter which may involve either or both pathways depending on the feed conditions. Experiments focused on the existence of the double peak feature at al low (240 °C), intermediate (330 or 370 °C), and high (484 °C) temperatures, as well as the reactivity of surface intermediates with O_2 and NO provide mechanistic insight. Based on the findings, a plausible reaction pathway involving HC-intermediates is proposed and its significance discussed.

2 Experimental Setup

2.1 Catalysts

A model LNT catalyst (provided by BASF, Iselin, NJ) consisting of 90 g/ft^3 precious group metal (PGM) with Pt/Rh mass ratio of 8:1, 15 wt% barium oxide and 34 wt% cerium oxide, and balance γ-Al_2O_3 was used in this study. The monolith catalyst was cut from a larger cylindrical core having a cell density of 400 CPSI (cells per square inch) and had a 4.6 g/in^3 washcoat loading. The monolith catalyst comprised ~ 55 channels and had a diameter (d) of 0.42 inch (1.07 cm) and a length (L) of 1 inch (2.54 cm). In order to simulate ~ 160,000 km aging, the catalyst sample was aged at 700 °C in air for 33 h before any performance evaluation, following the protocol reported by Toyota researchers [5].

2.2 Reactor System

The flow reactor setup used in this study is described elsewhere [27]. A solenoid-actuated four-way valve (Valco Inc., Micro-electric two position valve) enabled the HC pulsing via switching between lean and rich feeds. A syringe pump (Teleyne Isco model 100DX) and vaporization system delivered water to the feed gas. The effluent gas concentrations including NO, NO_2, N_2O, NH_3, and H_2O were monitored by a FTIR spectrometer (Thermo Scientific, 6700 Nicolet) which has a 200 ml gas cell. A quadrupole mass spectrometer (QMS) monitored the m/e = 28 signal. Temperatures were measured at selected points in the reactor system with strategically-placed K-type, stainless steel sheathed thermocouples (Omega Engineering).

Insight about the reaction pathways can be obtained by monitoring the N_2 generation throughout the entire cycle. This was accomplished with the QMS in combination with the FTIR. The QMS-measured m/e = 28 signal was used as a semi-quantitative indicator of overlapping species N_2, N_2O, CO, and CO_2 (secondary peak), while FTIR was used to independently measure the N_2O, CO, and CO_2 concentration. Differences in the transient response of the QMS and FTIR due to downstream mixing effects in the latter prevented a precise comparison; we elaborate on this point below, as is the estimation of the contributions of N_2, N_2O, CO, and CO_2 to the m/e = 28 signal. The QMS background signal was determined during the flow of Ar only in most experiments. When the feed contained CO_2 the background corresponded to a Ar/CO_2 mixture with the CO_2 concentration equal (5% $CO_2 = 25 \times 10^{-10}$ Torr). The timing of the QMS and FTIR were synchronized by matching the QMS m/e = 28 signal and FTIR N_2O signal during the switch from lean to rich period. The QMS was sensitive to pressure changes during this switch and resulted in a minor peak ($< 0.4 \times 10^{-10}$ Torr) right after the switch.

Differences in the transient response of the QMS and FTIR complicated the assessment of species contributions to the m/e = 28 peak. Our estimates of the response time for the QMS and FTIR are < 1 and ~ 4 s, respectively [9]. Thus, even a calibrated QMS may be misleading. For this reason, we report only the QMS-measured partial pressure of the m/e = 28 signal. Then through the aforementioned time synchronization of the QMS and FTIR measurements we can assess the contribution of N_2O, CO and CO_2 to the m/e = 28 signal. This is critical for evaluating the generation of N_2 during the early lean period in particular. As described below, this approach is particularly revealing for experiments in which the FTIR-measured N_2O, CO and CO_2 concentrations are low over the time period of interest.

Several feed mixtures were used and are detailed in Table 1. In Set I, the rich feed comprised two types; the "aerobic rich feed contained" 9% H_2/1% C_3H_6, and 2.5% O_2 while the "anaerobic rich feed" contained 4% H_2/0.45% C_3H_6, and 0% O_2. The reductant concentrations for the latter were selected based on complete consumption of 2.5% O_2 in the former experiments; in so doing this gave equal levels of "excess" reductant as quantified by the rich (R) feed stoichiometric number, $S_{N,R}$, given by.

$$S_{N,R} = \frac{2[O_2] + [NO]}{[CO] + [H_2] + 9[C_3H_6] - 2[O_{2,R}]}, \quad (1)$$

where for example, $[O_{2,R}]$ is the O_2 concentration in the rich feed. The choice of the two feeds is described in more detail in the Sect. 3. The lean feed also contained 5% O_2, 500 ppm NO, 0/3.5% H_2O and 5% CO_2 while both rich feeds contained the same concentrations of NO, H_2O, and CO_2. The Set II feed was the same as Set I except for 1000 ppm NO, 0% H_2O and 0% CO_2.

Two different timing protocols were used to study the injection frequency impact: 60 s lean/10 s rich (60/10) and 6 s lean/1 s (6/1) rich. Prior to each set of experiments, the catalyst was pretreated at 400 °C for 15 min to 30 s lean/5 s rich and 6 s lean/1 s rich conditions, respectively. For each experimental set, a cyclic steady state was reached typically within 30 min.

Since the aim of this study is to evaluate the existence and reactivity of surface HC-intermediates, the focus was on the early lean period during which HC-intermediates had been just formed and then exposed to an oxidizing atmosphere. The data during the rest of the cycle, shown for completeness, provide insight about the comparative behavior of the different reductants.

3 Results

3.1 Double Peaks with Anaerobic Rich Feed Without CO_2

Figure 1 compares the QMS-measured m/e = 28 signal, along with the FTIR-measured CO, CO_2, and N_2O effluent concentrations, with H_2 (blue) and C_3H_6 (red) as sole reductants for a slow-cycling (60/10) feed at temperatures of 240, 330, and 484 °C. The rich feed is anaerobic and without H_2O or CO_2, i.e. feed Set 2 in Table 1.

When using H_2 as reductant, the m/e = 28 signal appears during the first 5 s of the rich feed. There is also a small peak occurring just after the switch from rich to lean feeds. The corresponding FTIR CO and CO_2 concentrations are negligible (as expected) during the entire cycle (not shown), implying that N_2 is the sole m/e = 28 species. Following the conventional NSR mechanism, the N_2 forms from the reduction of stored NOx [28]. With increasing feed temperature, the intensity of the primary peak decreases. This is attributed to a decreasing NOx storage capacity and increasing NH_3 selectivity with temperature [9]. The second, minor peak results from the pressure change during the switch as mentioned previously.

In contrast, when using C_3H_6 as the reductant, two m/e = 28 peaks are detected for each of the feed temperatures. At 240 and 330 °C, the primary peak spans the entire rich period with a maximum occurring within the first 5 s, while the second peak appears after the feed switch from rich to lean. At 484 °C, two shallower peaks occur during the rich period. The lean feed m/e = 28 peak is likely a result of species generated from the oxidation of adsorbed intermediates. These unidentified species accumulate during their generation from reaction between C_3H_6 and stored

Table 1 Experimental conditions and catalyst properties

Experimental conditions	Set 1 Aerobic	Set 1 Anaerobic	Set 2
GHSV (1/h)	74,000	74,000	74,000
Cycle time (s)	60/10, 6/1	60/10, 6/1	60/10, 30/5, 6/1
Lean feed	5% O_2		
Rich feed	2.5% O_2 9% H_2/ 1% C_3H_6	0% O_2 4% H_2/ 0.45% C_3H_6	0% O_2 4% H_2/ 0.45% C_3H_6
Both feeds	500 ppm NO 5% CO_2 0/3.5% H_2O		1000 ppm NO 0% CO_2 0% H_2O
Catalyst properties			
L (cm)	2.54		
PGM (g/ft^3)	90		
BaO (wt%)	15		
CeO_2 (wt%)	34		

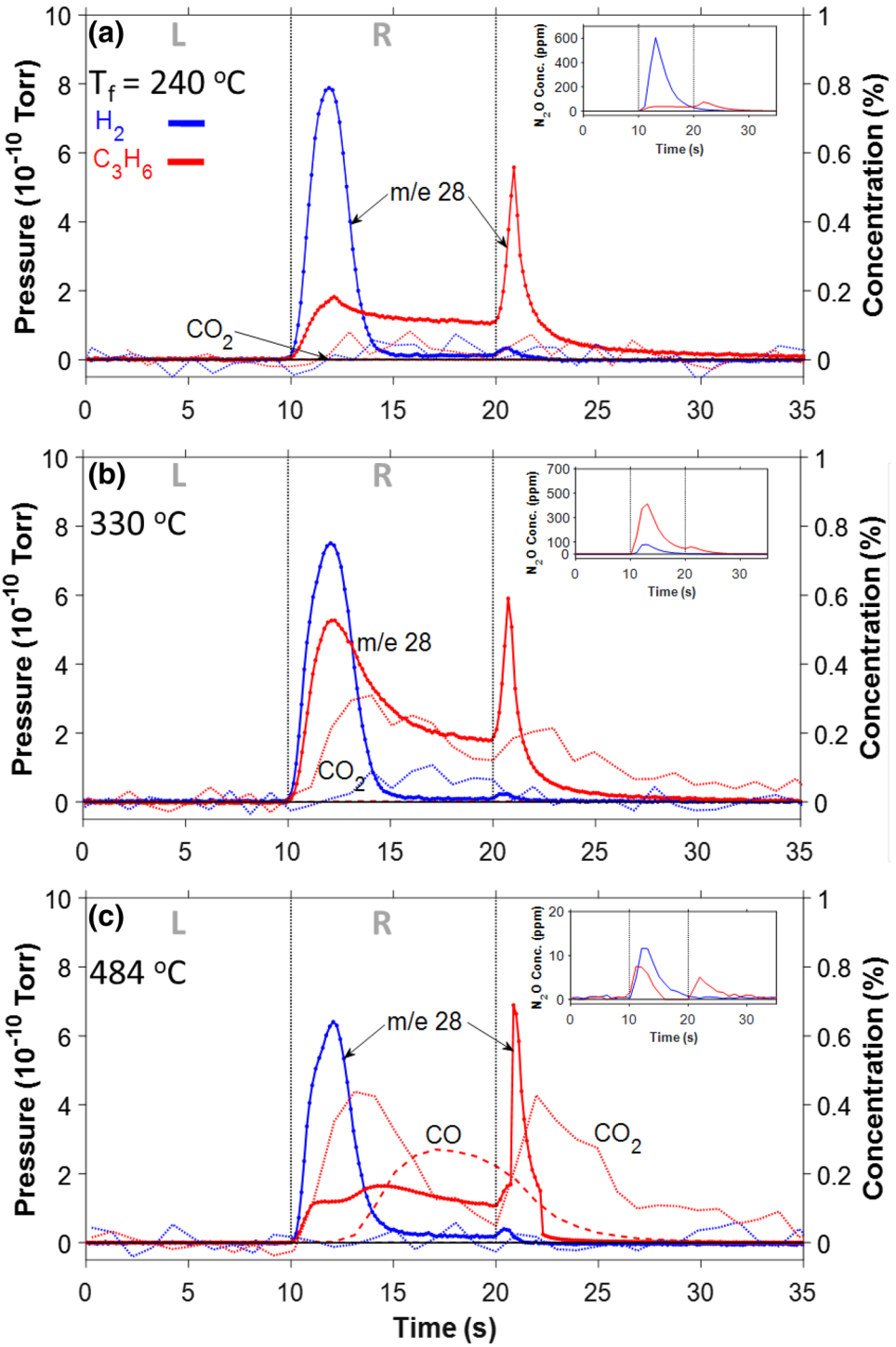

Fig. 1 Comparison of m/e 28 signal (solid line with circle marker) from mass spectrometer, CO (dashed line) and CO_2 (dotted line) and N_2O (corner subplot) effluent concentration from FTIR between using H_2 (blue) and C_3H_6 (red) as reductants at 240 (**a**), 330 (**b**), and 484 (**c**) °C feed temperatures under slow cycling (60/10) with anaerobic rich feed. Feed condition is as set 2 in Table 1. [m/e = 28 signal for C_3H_6 is divided by 5 at 484 °C]

NOx during the rich feed [7]. Two peaks of CO_2 are noted at 330 °C and 484 °C, one during the rich feed and the other during the lean feed. These are likely a result of the oxidation of the C_3H_6 during the rich feed and HC-intermediates during the lean feed. Reduction of stored and fed NO by C_3H_6 occurs during the early rich period, while oxidation of HC-intermediates by O_2 occurs during the early lean period. Finally, a CO peak occurs only at 484 °C, likely from the partial oxidation of C_3H_6 by ceria oxide. We expand more on the latter point below [29].

The inset plots in Fig. 1 compare N_2O generated with the two reductants. When using H_2, only one peak of N_2O is observed during the rich feed for all three feed temperatures. The magnitude of N_2O decreases from 600 to 80 and to 12 ppm as the feed temperature increases from 240 to 330 and to 484 °C. In contrast, for C_3H_6, two peaks of N_2O are

detected at all feed temperatures. The first N_2O peak spans the entire rich feed and is sustained at ~40 ppm at 240 °C and a more intense peak of ~400 ppm is obtained at 330 °C, while at 484 °C the N_2O peak is ~7 ppm. A second N_2O peak is detected for each feed temperature, with the peak at ~70 ppm at 240 and 330 °C, and at ~5 ppm at 484 °C. This N_2O secondary peak is likely generated from reactions between adsorbed intermediates and residual stored NOx [22].

Figure 2 compares the QMS m/e = 28 signal, and the FTIR CO and CO_2 effluent concentrations when using H_2 (blue) and C_3H_6 (red) as the reductant. In these experiments, the feed temperature is 484 °C and the cycle time is 30/5 (a) and 6/1 (b); the 60/10 data are shown in Fig. 1c. Only one prominent m/e = 28 peak is detected when using H_2 for each of the cycle times. Complex, multi-peak features are seen with C_3H_6. For example, for the 30/5 cycle, two peaks are clearly evident during the rich period and a third peak is observed during the lean feed. The lean feed peak was also encountered for the slower 60/10 cycle, and appears coincidentally with a CO_2 peak. The fast cycling 6/1 data show a single m/e = 28 peak that appears during the rich period and extends into lean period. These trends are discussed later in terms of the underlying reaction pathways.

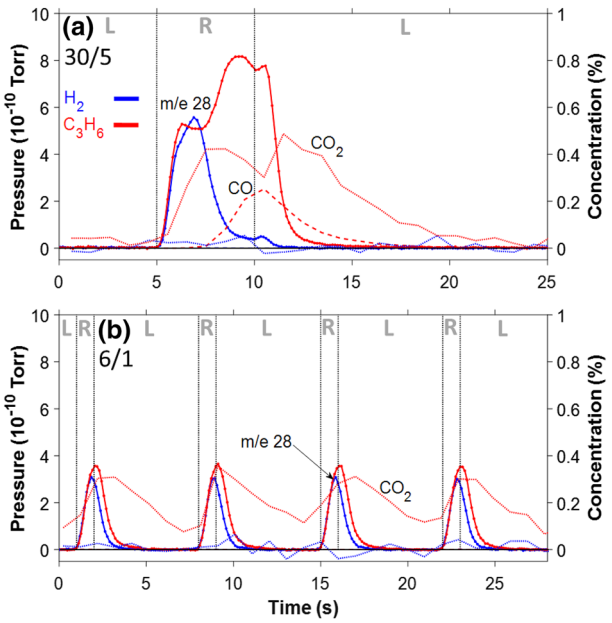

Fig. 2 Comparison of m/e 28 signal from mass spectrometer, CO and CO_2 effluent concentration from FTIR between using H_2 (blue) and C_3H_6 (red) as reductants at 484 °C feed temperature under cycle times of 30/5 (**a**) and 6/1 (**b**) with anaerobic rich feed. Feed condition is as Set 2 in Table 1

3.2 Double Peak with Anaerobic Rich Feed with CO_2

Similar experiments were carried out with 5% CO_2 included in the lean and anaerobic rich feeds. The presence of the feed CO_2 results in CO formation; this complicates the data analysis as discussed below. Figure 3 compares the m/e = 28 (N_2, CO, CO_2) along with the FTIR CO and N_2O effluent concentrations for H_2 (blue) and C_3H_6 (red) at 240, 370, and 483 °C during slow cycling (60/10) with an anaerobic rich feed. Both reductants show double peaks for the m/e = 28 signal but at different feed temperatures. For H_2, the second peak is prominent at 240 °C, while for C_3H_6 the second peak occurs at 370 and 483 °C feed temperatures. For both reductants, the rich feed peak is followed by a plateau spanning the remainder of the rich period that extends for a few seconds into the lean period.

These data are more difficult to decipher than the CO_2-free data of Fig. 1 since CO is detected for all temperatures (for H_2) and at 483 °C (for C_3H_6). Its origin in the H_2 reductant experiments is via the reverse WGS reaction:

$$H_2 + CO_2 \leftrightarrow CO + H_2O, \quad \text{(R1)}$$

while for the C_3H_6 reductant experiments CO is likely formed via propylene partial oxidation with O_2 or oxidation by ceria-supplied stored oxygen:

$$C_3H_6 + 1.5O_2 \leftrightarrow 3CO + 3H_2, \quad \text{(R2)}$$

$$C_3H_6 + 3Ce_2O_4 \leftrightarrow 3CO + 3H_2 + 3Ce_2O_3, \quad \text{(R3)}$$

Dry reforming of propylene may also contribute:

$$C_3H_6 + 3CO_2 \leftrightarrow 6CO + 3H_2, \quad \text{(R4)}$$

The inset plots in Fig. 3 compare the N_2O effluent data for each of the experiments. For C_3H_6, secondary N_2O peaks of 75 and 20 ppm are detected at temperatures of 240 and 370 °C, respectively; however, double peaks of N_2O are only observed at 240 °C for the case of H_2. A negligible amount of N_2O is detected at 483 °C.

3.3 Reactivity of HC-Intermediates

A key mechanistic issue regards the existence and reactivity of hydrocarbon surface intermediates when using a hydrocarbon reductant. In order to probe this issue, a series of experiments were carried out to provide evidence, albeit indirect, for reactive surface HC species. Our approach was to subject the catalyst to the conventional slower lean-rich cycle (60/10 timing). Upon establishing a cyclic steady state, at the end of the final rich pulse the catalyst was exposed to an inert atmosphere (Ar only) of varying duration. The effluent was analyzed with the QMS and FTIR throughout the experiment. In discussion which follows, notation is used to depict the feed sequence of varying duration as $10/t_I/(80-t_I)$ corresponding to Rich/Inert/Lean, where t_I represents the

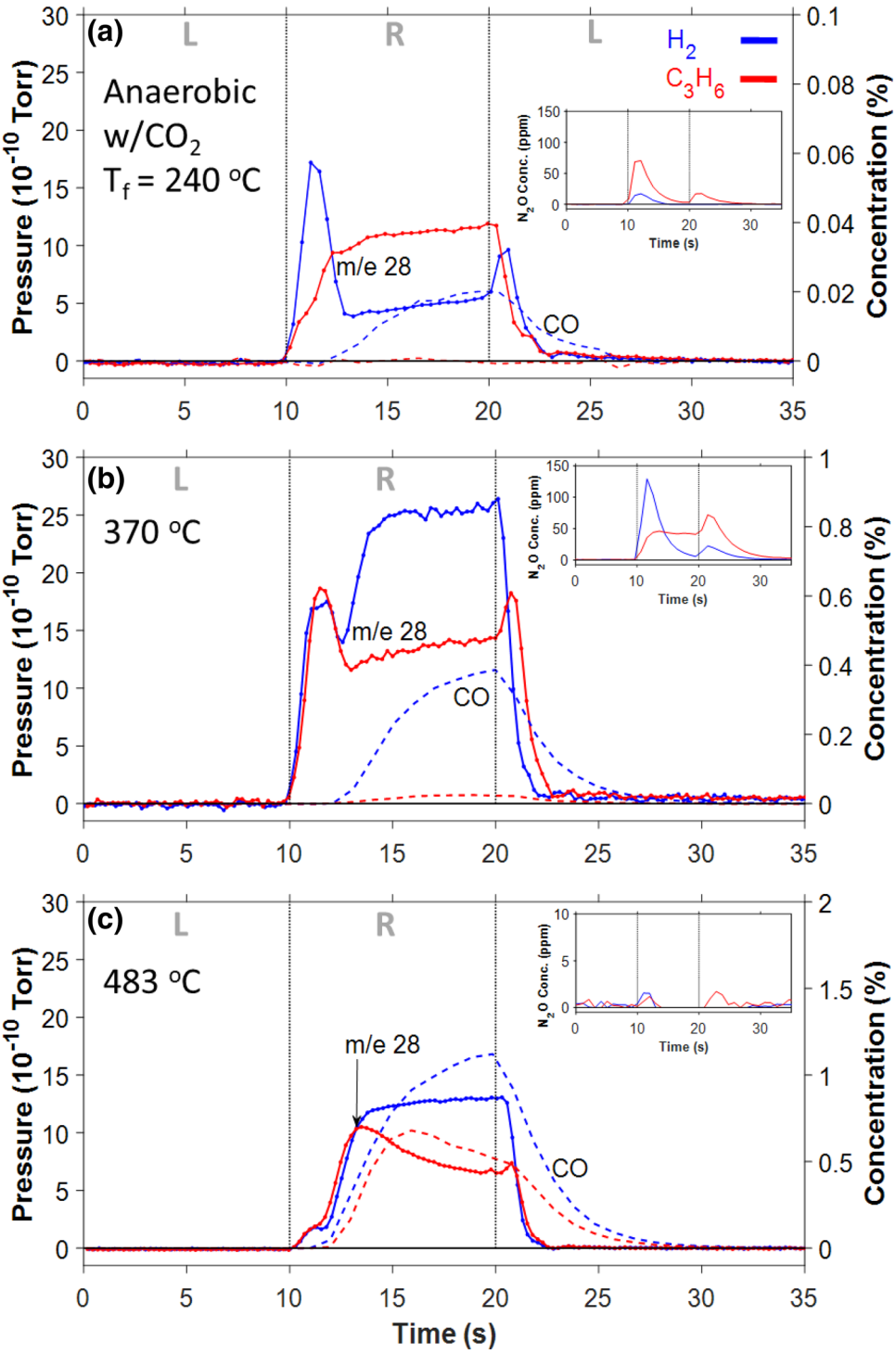

Fig. 3 Comparison of m/e 28 (solid line with circle marker) from mass spectrometer, CO (dashed line) and N_2O effluent concentration from FTIR between using H_2 and C_3H_6 as reductants at 240 (**a**), 370 (**b**), and 484 (**c**) °C feed temperatures under slow cycling (60/10) with anaerobic rich feed in the presence of 5% CO_2. Feed condition is as Set 1 in Table 1

duration of the Inert feed; e.g. 10/20/60 corresponds to a 60/10 lean-rich cycle that has reached cyclic steady state that is followed by a 20-s Inert feed. In the set of experiments to be described the 484 °C rich feed is anaerobic and devoid of CO_2. N_2O is negligible (< 5 ppm) at this high temperature.

Figure 4 shows the QMS-measured m/e = 28 signal (a), and the FTIR-measured CO, C_3H_6 (b) and CO_2 (c) concentrations during this series of experiments in which the Inert feed duration was varied from 0 to 30 s. The 10/0/80 data (last peak to the right in Fig. 4a) shows the expected result (Fig. 4a); i.e., a dual m/e = 28 peak, generation of CO with breakthrough of unreacted C_3H_6 (Fig. 4b), and a dual CO_2 peak (Fig. 4c). As the duration of the Inert feed was increased from 0 to 30 s (right to left in Fig. 4a), the second

peak decreased in intensity while a decaying tail emerged between the first and second peaks. Finally, for the longest duration Inert experiment of 30 s, only a single peak and decay feature was measured.

These data clearly show a persistent but decreasing magnitude of the m/e = 28 signal upon the introduction of the lean feed. Interpretation of this trend depends on a reliable assessment of the relative contributions to the m/e = 28 peak by N_2, CO_2, CO, and N_2O. This is accomplished through examination of the FTIR-measured concentrations of the latter three species. We consider each one-by-one.

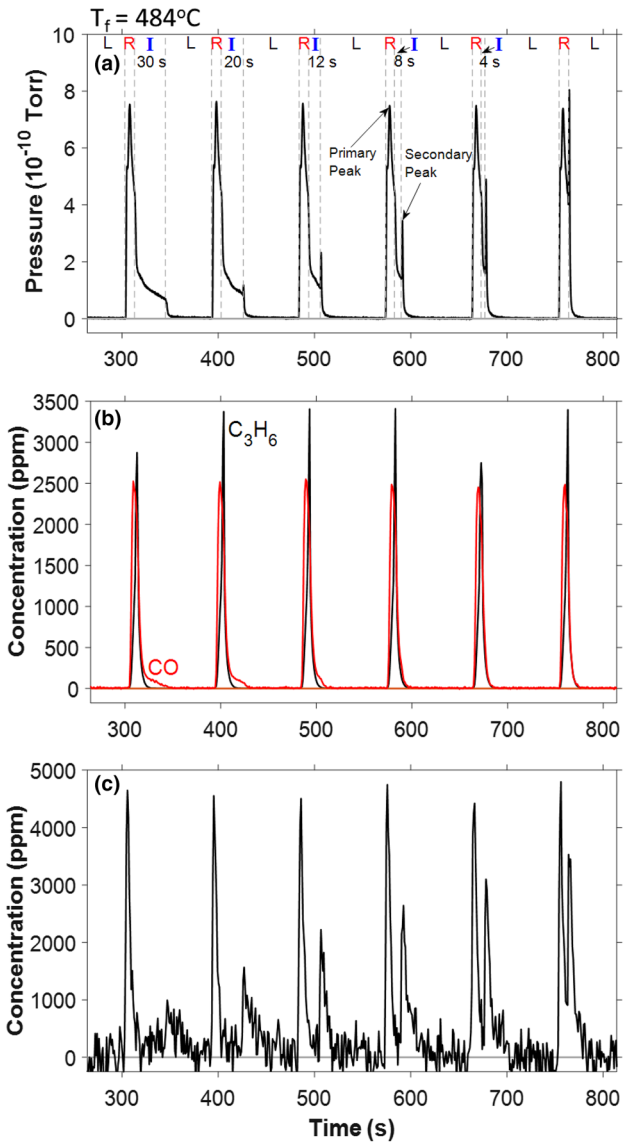

Fig. 4 The m/e 28 signal from mass spectrometer (**a**), CO and C_3H_6 (**b**), and CO_2 (**c**) effluent concentration from FTIR at 484 °C feed temperature under cycle times of 10/30 ~ 0/50 ~ 80 s (Rich, Inert, Lean,) with lean and rich feed described in set 2 in Table 1

Regarding CO, Fig. 4b shows that CO was detected during the short rich period, with maximum concentration of ~ 2500 ppm. There is also a short-lived tail that coincides with the m/e = 28 tail. However, upon the switch from the Inert to lean feed there is no detectable second peak. This rules out a contribution of CO to the second m/e = 28 peak.

Regarding N_2O, its contribution to the second peak is also negligible. For N_2O the relative intensity of the m/e = 28 to the parent m/e = 44 peak is ~ 15% [30]. Fig. S1 provides the N_2O mass spectrum. More importantly, with C_3H_6 as the reductant, the maximum N_2O concentration measured with the FTIR was ~ 5 ppm at 484 °C (Fig. 1a). At these temperatures N_2O formation is known to be negligible due to the N–O bond scission [31]. This amount is small and negligible.

Unlike CO and N_2O, the third non-N_2 component, CO_2, cannot be ruled out as contributing to the second m/e = 28 peak. The extent of its contribution relies on comparison of the intensity of the m/e = 28 s peak along with the FTIR-measured concentration. As shown in Fig. S2 in Supplementary Material, the CO_2 concentration increases linearly with the decreasing Inert feed duration, while the m/e = 28 signal increases non-linearly. With the CO^+ peak of CO_2 linearly dependent on the CO_2 concentration, this implies that the only remaining m/e = 28 component is N_2^+. Thus, the surface species contains both N and C, and likely H and O, and during exposure to O_2 generates a mixture of N_2 and CO_2. Furthermore, Fig. S2 shows that there is less N_2 contribution to the secondary peak in the longer duration Inert feed experiments. This suggests that the decaying m/e = 28 tail observed during the Inert feed also contains N_2 in order to satisfy the N balance. The implications of these findings to the underlying reaction pathways will be addressed in the Sect. 4.

Figure 5 shows another set of experiments in which the catalyst was first exposed to Ar, then O_2 (5% in Ar) or NO (1000 ppm in Ar), followed by a conventional 60/10 lean/rich cycle. The sequence was run at least three times to establish repeatable results. The notation 11/10 O_2/59/10 corresponds to an 11 s Inert, 10 s O_2/Ar, then a 59/10 lean rich cycle. Experiments with reductants H_2 (blue) and C_3H_6 (red) are compared. The rich feeds are anaerobic and devoid of CO_2. Experiments in Fig. 5a, d correspond to 20/0/60/10 s, Fig. 5b, e correspond to 11/10 O_2/59/10, while Fig. 5c, f correspond to 11/10 NO/59/10. Figure 5a–c show the effluent QMS m/e = 28 signal, and (d–f) show the CO and CO_2 FTIR concentrations when using C_3H_6.

With H_2 as the reductant only one m/e = 28 peak (blue) is seen at the beginning of the rich period for the inert Ar and Ar + O_2 exposure experiments (blue curves in Fig. 5a, b). During the Ar + NO exposure experiment a second peak with a plateau is evident (Fig. 5c). In contrast, multiple peaks are seen with C_3H_6 for each of the three experiments. As seen in

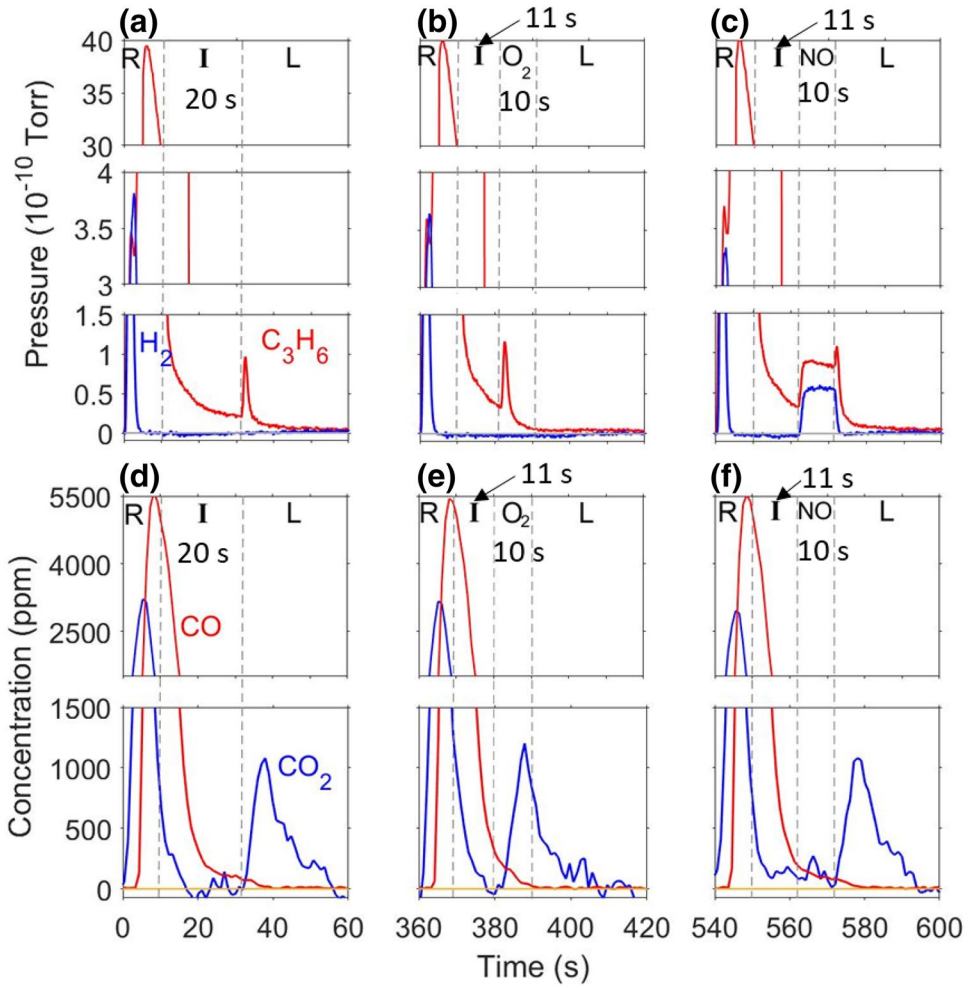

Fig. 5 Comparison of m/e 28 signal **a**–**c** from mass spectrometer between using H_2 (red) and C_3H_6 (blue) as the reductant, and CO (red), and CO_2 (blue) effluent concentration from FTIR for C_3H_6 only **d**–**f** at 525 °C feed temperature under cycle times of 20/0/60/10 s (Inert, 5% O_2 or 1000 ppm NO only, Lean, and Rich) for **a** and **d**, 11/10 O_2/59/10 for experiments **b** and **e**, and 11/10 NO/59/10 for experiments **c** and **f** with lean and rich feed described in set 2 in Table 1

Fig. 5a, a decaying signal exists during the Inert feed period, and an abrupt peak appears right after the switch from rich to lean period (as is reported in reference to Fig. 4a). Figure 5b shows that when the Inert feed is replaced with a 10 s O_2/Ar feed this gives a shorter decay period with the peak evident at the onset of the O_2/Ar feed. As seen in Fig. 5c, when a 10 s NO/Ar feed replaces the O_2/Ar feed, the decaying signal is still 10 s long, but a nearly constant m/e = 28 signal exists when only NO is fed. The peak occurs at the beginning of the lean period as in Fig. 5a. Examination of Fig. 5d, e show a correspondence of CO_2 production (peaks) with the m/e = 28 peaks reported in Fig. (a, b), respectively. This is consistent with earlier data (Fig. 4). Similar trends are seen in comparing Fig. 5c, f for the Ar/NO experiment. The lack of CO_2 evolution during the NO exposure is negligible, in stark contrast to the O_2 exposure in Fig. 5b, e. We expand on this point in Sect. 4.

3.4 Analysis of m/e = 28 Under Fast Cycling

As discussed earlier, the enhancement in NOx conversion with fast injection of C_3H_6 is a result of more effective stored NOx utilization contribution by oxidation a surface N-containing oxygenate. In addition, a large temperature rise may be encountered during HC injection into a feed containing O_2 [9]. It is therefore of interest to follow the evolution of the m/e = 28 signal using an aerobic rich feed during fast cycling. It is noted that N_2O is negligible under fast cycling at 370 and 483 °C (not shown here).

Figure 6 compares the m/e = 28 signal and CO concentration for experiments with reductants H_2 (blue) and C_3H_6 (red) at feed temperatures of 240 (6.a), 370 (6.b), and 483 °C (6.c) during fast cycling (6/1), and with an anaerobic rich feed containing 5% CO_2. For all feed temperatures, a negligible amount of CO was detected by the FTIR and therefore the m/e = 28 peak is attributed to N_2. The m/e = 28 signal appears during the reductant injection and extends into the lean period for both reductants for each of the feed temperatures. At 240 °C, the smaller

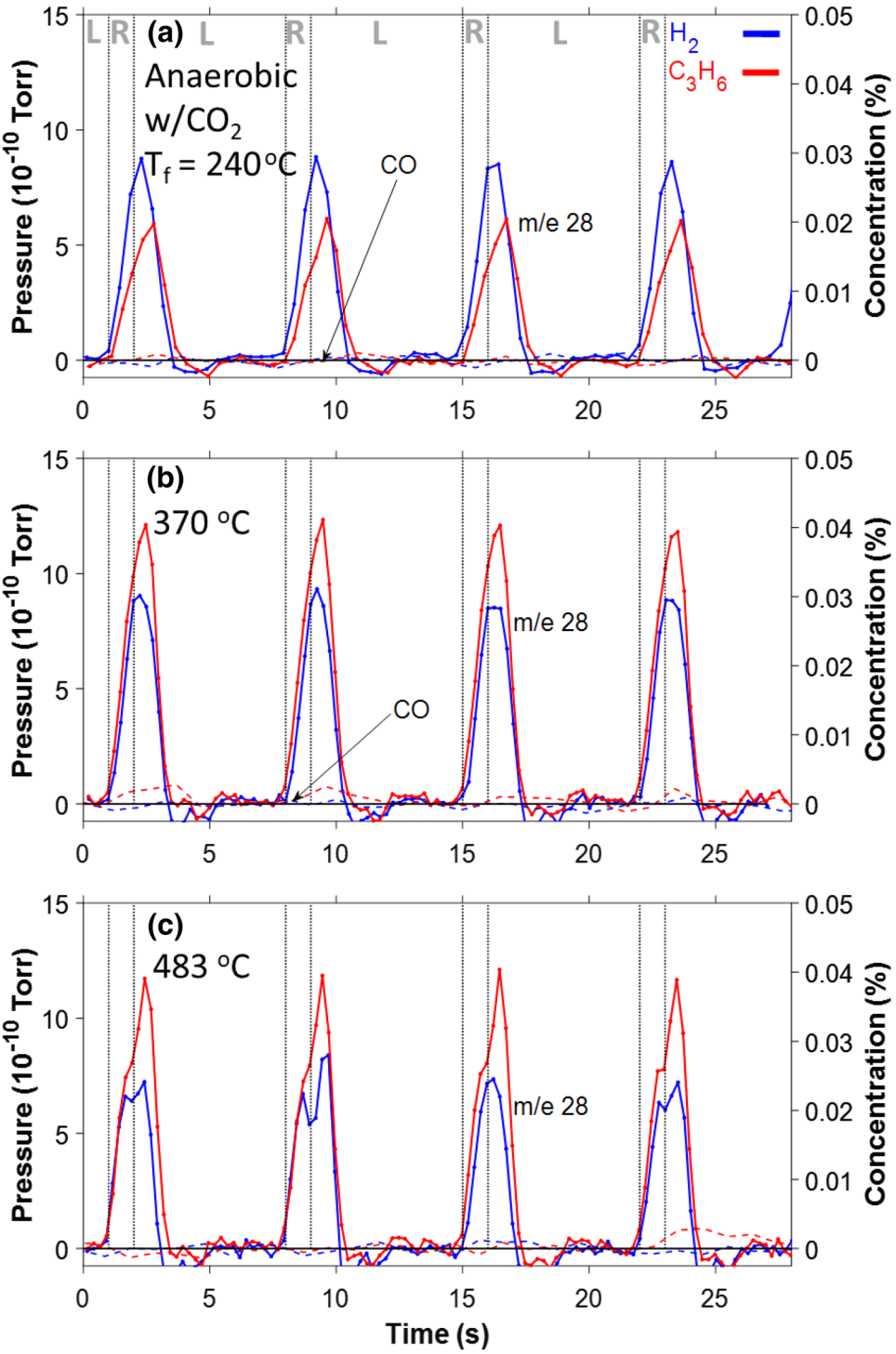

Fig. 6 Comparison of m/e 28 signal from mass spectrometer, CO effluent concentration from FTIR between using H_2 and C_3H_6 as reductant s at 238 (**a**), 370 (**b**), 483 °C (**c**) feed temperatures under cycle times of 6/1 with anaerobic rich feed and in presence of 5% CO_2. Rich period is enclosed within two vertical bars. Feed condition is as aerobic set 1 in Table 1

m/e = 28 peak obtained for C_3H_6 is attributed to its lower reactivity which lessens the extent of NOx reduction. In contrast, at the higher temperatures of 370 and 483 °C, reduction by C_3H_6 gives a more intense m/e = 28 signal than by H_2. There is some indication of a split peak at 483 °C with H_2.

Figure 7 shows analogous data for the aerobic rich feed. For H_2, the m/e = 28 peak is similar to that obtained under anaerobic conditions (Fig. 6), although the peak is ~ 20–30% higher. This is explained in part by the exotherm from H_2 oxidation which increases the catalyst temperature by 60–100 °C [9]. CO formation also increases due to the partial oxidation of C_3H_6 although

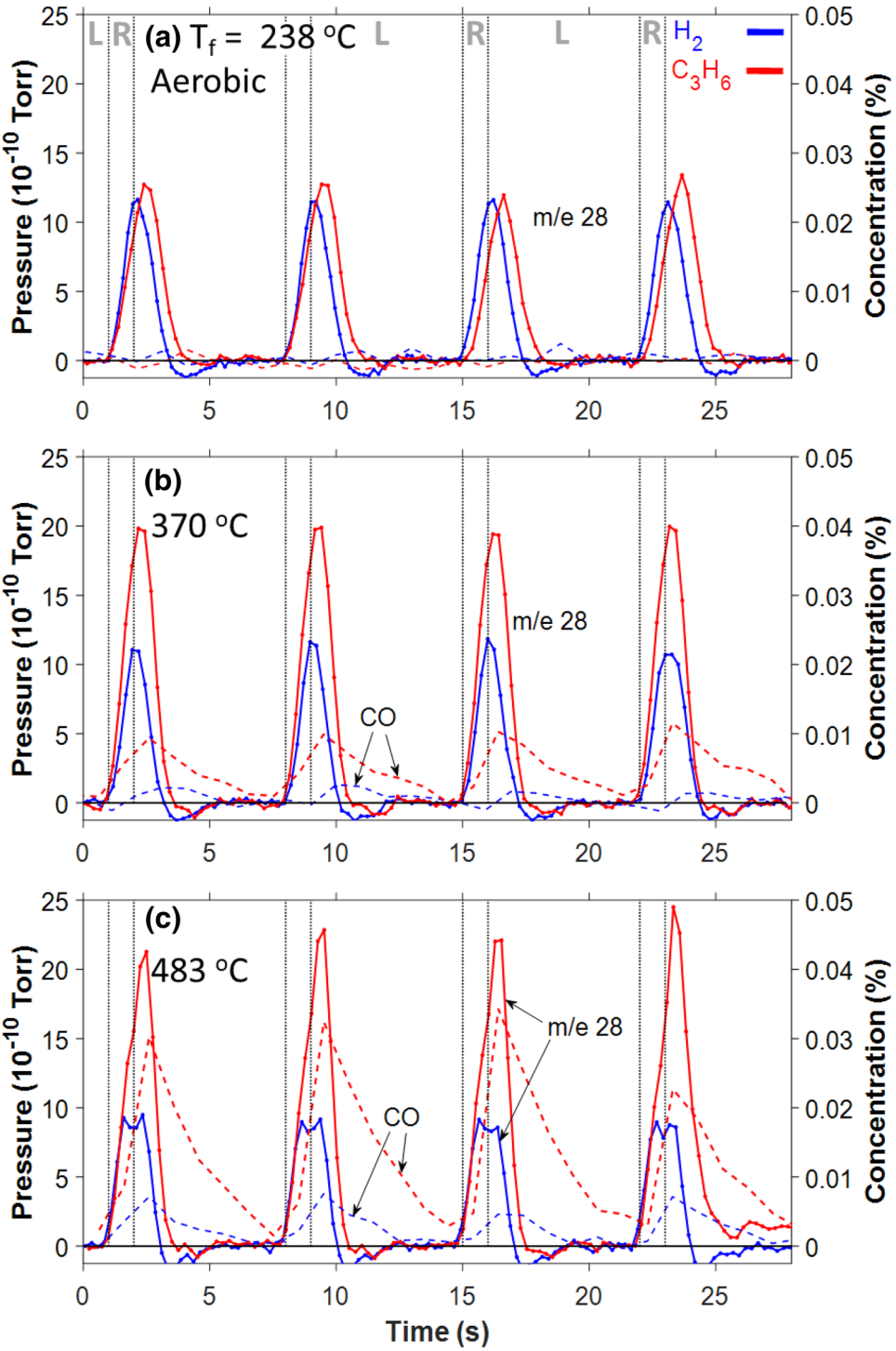

Fig. 7 Comparison of m/e 28 signal from mass spectrometer, CO effluent concentration from FTIR between using H_2 and C_3H_6 as reductants at 238 (**a**), 370 (**b**), 483 (**c**) °C feed temperatures under cycle times of 6/1 with aerobic rich feed and in presence of 5% CO_2. Rich period is enclosed within two vertical bars. Feed condition is as aerobic set 1 in Table 1

the CO concentration does not exceed 350 ppm. Similarly, the m/e = 28 peak obtained with C_3H_6 is more intense than that obtained with the anaerobic feed. The exotherm increases the temperature by 20 and 90 °C at 238 and 370 °C feed temperatures, respectively. This temperature rise helps to mitigate the inhibition effect, generating more N_2 through a faster regeneration rate. Overall, C_3H_6 is the more effective reductant for the aerobic feed as indicated by the more intense m/e = 28 peak.

4 Discussion

Detailed features of the reacting and product species concentrations during lean-rich switching provide evidence for competing NOx reduction pathway(s). The conventional NSR performance features and mechanism is by now well established in the literature and is briefly summarized here. With H_2 as the reductant and in the absence of CO_2, generation of N_2 and N_2O occur during the first part of the rich feed, followed by NH_3 during the latter part [32]. The emergence of NH_3 after N_2 is a result of the depletion of stored NOx through reaction with H_2 upstream and NH_3 downstream. No N_2 is detected during the lean feed of the cycle. Moreover, NOx stores as nitrites [$Ba(NO_2)_2$] and nitrates [$Ba(NO_3)_2$] through reaction with BaO, $Ba(OH)_2$.

The introduction of CO_2 to the feed leads to the formation of $Ba(CO_3)_2$ which is more stable than $Ba(OH)_2$ and BaO [17, 24]. This results in a lower NOx storage capacity for a given temperature [33]. In addition, a second peak of N_2 may appear during the lean part of the cycle. This is a result of participation of surface isocyanates [24]. With CO_2 in the feed, CO is formed via the reverse WGS reaction (R1). CO itself participates in NOx reduction through Pt-catalyzed reaction of adsorbed CO and NO, leading to the formation of N_2 and N_2O. Another route involves the formation of surface isocyanates NCO-X [6, 23–26], which may accumulate on both the Pt and adjacent BaO and CeO_2 surfaces. As a result, oxidation of the isocyanate may occur during the lean feed; potential surface reactions include the following:

$$\text{NCO-X} + 0.5O_2 \rightarrow 0.5N_2 + CO_2 + \text{X} \quad \text{(R5)}$$

$$\text{NCO-X} + 0.75O_2 \rightarrow 0.5N_2O + CO_2 + \text{X} \quad \text{(R6)}$$

where X denotes a binding site. Several studies have reported the second N_2 and/or N_2O peak during the lean feed of the cycle when CO is present. Expanding on this point, double peaks of N_2, N_2O and CO_2 are evidence of an alternative NOx reduction pathway involving HC intermediates, isocyanates, etc. The double peaks are generally thought to occur during the switch from rich to lean involving reactions like (R5) and (R6).

Most researchers to date have reported double peaks at temperatures below 350 °C, with anaerobic rich feeds, and for conventional NSR cycle times of 1 min and rich injection times of several seconds or longer. In the current study, double peaks were observed over a more diverse set of conditions, including not only anaerobic rich feeds at low to intermediate temperature, but also aerobic rich feeds at high temperature. For example, prominent double peaks of N_2, CO_2, and N_2O were encountered at 484 °C using an anaerobic feed and the 70 s (60/10) cycle (Fig. 1c). The double peak feature is sustained as the cycle is shortened from 70 to 35 s (Fig. 2a). And while only a single peak is evident during the 7-s cycle (Fig. 2b), N_2 production persists into the first part of the lean feed and infer the persistence of the reaction pathway. These and other data suggest that involved intermediates are sufficiently stable under these conditions to participate in the NOx reduction. Adsorbed NCO is certainly not stable. Alternatively, intermediates such as organo-isocyanates (R-NCO) and nitriles (R-CN) which have been observed during high temperature DRIFTS. While the actual identity of these species is not known, the mass spectrometer and FTIR measurements confirm that the species contain C, N, and possibly H and O atoms, so that their reaction with oxygen leads to the products CO_2, N_2, and N_2O.

Prior to the current study, a double peak of N_2 has not been reported for shorter cycle times. Figures 1c and 2 compare the m/e = 28, CO and CO_2 for different cycle time at 484 °C with an anaerobic rich feed. Only one peak was detected when using H_2. In contrast, when using C_3H_6 during both 60/10 and 30/5 cycling, double peaks for m/e = 28 and CO_2 occurred during the lean feed. While only one peak was observed during the faster 6/1 switching experiment, the data show evidence for N_2 formation during the lean period. Detection of one extended peak, instead of two peaks, may be a result of upstream mixing.

The double peak behavior encountered with an aerobic rich feed containing CO_2, and over a wide range of temperatures (Fig. 3) points to the existence of two NOx reduction paths. The double peak of m/e = 28 detected at 240 °C when using H_2 in the presence of CO_2 is likely via the aforementioned isocyanate (NCO-X) pathway as no such lean feature is evident in the absence of feed CO_2 (Fig. 1). This result is similar to that reported elsewhere [22, 25]. However, that the m/e = 28 and N_2O double peaks decrease in intensity at 370 and 483 °C for H_2 but not for C_3H_6 suggests that the involved intermediate for the latter has a higher thermal stability than an NCO-type species.

Previous researchers have studied the possible reaction pathways of the isocyanate/HC intermediates [24–26]. The isocyanate species reacts with oxygen and produces CO_2 and N_2 with high selectivity [34], while the formation of N_2O may originate from the reaction between isocyanate species and residual stored NOx. The HC-intermediate mechanism advanced by Bisaiji et al. [35] suggests that surface intermediates react with NO in the lean period, forming N_2, resulting in a NOx reduction enhancement for temperatures exceeding 400 °C.

The adsorbed species reactivity experiments reported (Figs. 4, 5) suggest that surface intermediates have sufficient thermal stability to participate in NOx reduction at elevated temperature. The data show that the decomposition of surface intermediates may occur, forming N_2 and CO. As the Inert exposure is shortened, a second N_2 peak appears along with a CO_2 peak during the switch from rich

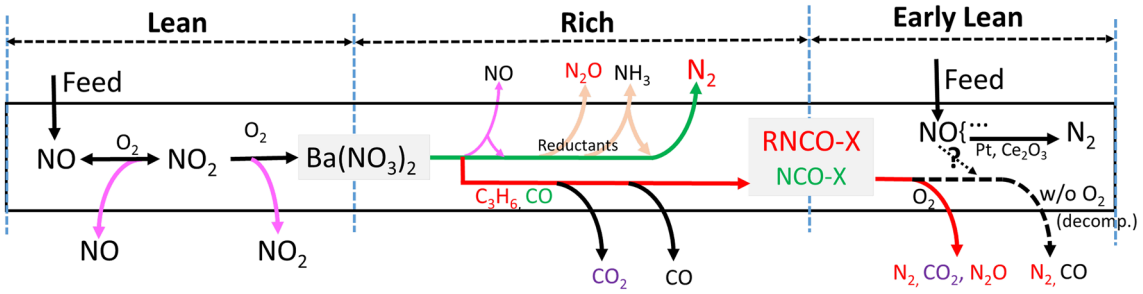

Fig. 8 Proposed general mechanism for NSR technology with H_2, CO, or C_3H_6 as reductants

to lean conditions. This observation suggests the following representative reactions for decomposition and oxidation:

$$\text{R-NCO} - \text{X} \rightarrow 0.5\text{N}_2 + \text{CO} + \text{R-X} \quad \text{(R7)}$$

$$\text{R-NCO} - \text{X} + 0.5\text{O}_2 \rightarrow 0.5\text{N}_2 + \text{CO}_2 + \text{R-X} \quad \text{(R8)}$$

where R is an alkyl group and X is a binding site. The data comparing H_2 and C_3H_6 (Fig. 5) clearly show peaks that involve hydrocarbon that are not present when using with H_2 as the reductant. Exposure to Ar only (Fig. 5a, d) shows the product of surface intermediate decomposition. The immediate emergence of the m/e = 28 peak (but no CO) during exposure of the adsorbed intermediate to O_2 (Fig. 5b, e) confirms the selective formation of N_2 and also suggests that NO is not required for N_2 formation. In contrast, the exposure to NO (Fig. 5c, f) leads to the N_2 plateau feature, while the secondary peak occurs right after the switch from NO-only to lean feed. The plateau of N_2 is also detected when using H_2, which suggests that the cause of the plateau is not likely from surface intermediates. Alternatively, N_2 may be formed through direct NO decomposition on reduced Pt sites [36] or reduced Ce sites [8]. Indeed, in Fig. 5f, CO_2 only corresponds to peaks at the beginning of rich and lean period, and reaction of isocyanate to NO must produce CO or CO_2, which are not detected during the 10 s NO feed.

In summary, these findings, suggest negligible reaction between the surface intermediates and NO:

$$\text{R-NCO} + \text{NO} \rightarrow \text{no reaction} \quad \text{(R9)}$$

while the formation of N_2 with NO-only feed is from the Pt or Ce catalyzed NO decomposition:

$$2\text{NO} + 2\text{Pt} \rightarrow \text{N}_2 + 2\text{Pt}-\text{O} \quad \text{(R10)}$$

$$2\text{NO} + 2\text{Ce}_2\text{O}_3 \rightarrow \text{N}_2 + 2\text{Ce}_2\text{O}_4 \quad \text{(R11)}$$

Surface hydrocarbon intermediates may thermally decompose to form N_2 and CO, but not CO_2 (R7), may be oxidized by O_2 to form N_2 (R8), without requiring NO (R9), and additional N_2 may be formed via NO decomposition (R10, R11). Combining existing traditional NSR technology and HC-intermediates NOx reduction pathway, the aforementioned reactions are shown in Fig. 8, this work proposed a general mechanism for NSR technology with H_2, CO, or C_3H_6 as the reductants.

5 Conclusions

An experimental study of fast cycling NOx storage and reduction with H_2 and C_3H_6 for emission control of lean burn gasoline and diesel vehicles was conducted to provide evidence for a HC-intermediate NOx reduction pathway. In order to differentiate the effect of HC-intermediate NOx reduction pathway on the NOx conversion from the effect of fast cycling, the experimental results using H_2 and C_3H_6 with the same lean/rich stoichiometry and under aerobic and anaerobic rich feed conditions were compared.

Using a combination of mass and FTIR spectrometry, double peaks of N_2, N_2O, and CO_2 has been treated as the evidence of formation of HC-intermediates [5, 7, 35]. The Di-Air mechanism proposed by Bisaiji et al. suggests that reduction of NO by adsorbed HC-intermediates (possibly R-NCO) in the early lean period, producing N_2 [7]. This work provides evidence for HC-intermediates in the presence of O_2, NO, and its thermal decomposition at different temperatures, over a range of different cycle times from ca. 1 min to ca. 5 s in duration with and without CO_2, and with aerobic/anaerobic conditions. Double peaks of N_2 and CO_2 detected in experiments under anaerobic rich feed conditions with cycle times of 60/10 and 30/5, without feed of CO_2 and H_2O, and when using C_3H_6, but not H_2. With H_2 as the reductant in the presence of CO_2 a double peak occurs at 240 °C, while with C_3H_6 at temperature as high as 484 °C suggests a surface HC species that is more stable than conventional isocyanate, formed from CO through reverse WGS reaction when using H_2. Lifetime experiments reveal that the thermal decomposition of R-NCO produces CO and N_2, while second peak upon switching to lean period indicates the oxidation of R-NCO by O_2 but not NO. Instead, NO decomposition is detected on reduced catalyst (Pt and Ce) sites under anaerobic conditions.

Acknowledgements This study was funded by grants from the U.S. DOE National Energy Technology Laboratory as part of the Vehicles Technologies Program DOE-NETL (DE-EE0000205) and National Science Foundation CBET 1258688.

References

1. Harold MP (2012) NOx storage and reduction in lean burn vehicle emission control: a catalytic engineer's playground. Curr Opin Chem Eng 1:303–311
2. Shakya BM, Harold MP, Balakotaiah V (2014) Modeling and analysis of dual-layer NOx storage and reduction and selective catalytic reduction monolithic catalyst. Chem Eng J 237:109–122
3. Zheng Y, Liu Y, Harold MP, Luss D (2014) LNT-SCR dual-layer catalysts optimized for lean NOx reduction by H_2 and CO. Appl Catal B Environ 148–149:311–321
4. Chen H-Y, Collier JE, Liu D, Mantarosie L, Durán-Martín D, Novák V, Rajaram RR, Thompsett D (2016) Low temperature NO storage of zeolite supported Pd for low temperature diesel engine emission control. Catal Lett 146:1706–1711
5. Bisaiji Y, Yoshida K, Inoue M, Umemoto K, Fukuma T (2011) Development of Di-Air—a new diesel de NOx system by adsorbed intermediate reductants. SAE Int J Fuels Lubr 5:2011-01-2089
6. Inoue M, Bisaiji Y, Yoshida K, Takagi N, Fukuma T (2013) DeNOx performance and reaction mechanism of the Di-air system. Top Catal 56:3–6
7. Uenishi T, Umemoto K, Yoshida K, Itoh T, Fukuma T (2014) Development of the design methodology f or a new De-NOx System. Int J Automot Eng 5:115–120
8. Wang Y, DeBoer JP, Kapteijn F, Makkee M (2016) Fundamental understanding of the Di-Air system: the role of Ceria in NOx abatement. Top Catal 59:854–860
9. Ting AWL, Li M, Harold MP, Balakotaiah V (2017) Fast cycling in a non-isothermal monolithic lean NOx trap using H_2 as reductant: experiments and modeling. Chem Eng J 326:419–435
10. Li M, Zheng Y, Luss D, Harold MP (2017) Impact of rapid cycling strategy on reductant effectiveness during NOx storage and reduction. Emiss Control Sci Technol 3:205
11. Perng CCY, Easterling VG, Harold MP (2014) Fast lean-rich cycling for enhanced NOx conversion on storage and reduction catalysts. Catal Today 231:125–134
12. Zheng Y, Li M, Wang D, Harold MP, Luss D (2016) Rapid propylene pulsing for enhanced low temperature NOx conversion on combined LNT-SCR catalysts. Catal Today 267:192–201
13. Li M, Easterling VG, Harold MP (2016) Spatio-temporal features of the sequential NOx storage and reduction and selective catalytic reduction reactor system. Catal Today 267:177–191
14. Reihani A, Fisher GB, Hoard JW, Theis JR, Pakko JD, Lamvert CK (2017) Rapidly pulsed reductants for diesel NOx reduction with lean NOx traps: effects of pulsing parameters on performance. Appl Catal B Environ 1–15
15. Reihani A, Patterson B, Hoard J, Fisher GB, Theis JR, Lambert CK (2016) Rapidly pulsed reductants for diesel NOx reduction with lean NOx traps: comparison of alkanes and alkenes as the reducing agent. J Eng Gas Turbines Power 139:102805
16. Ting AWL, Harold MP, Balakotaiah V (2018) Elucidating the mechanism of fast cycling NOx storage and reduction using C_3H_6 and H_2 as reductants. Chem Eng Sci
17. Burch R, Sullivan JA (1999) A transient kinetic study of the mechanism of the $NO/C_3H_6/O_2$ reaction over Pt-SiO_2 catalysts. Part I: Non-steady-state transient switching experiments. J Catal 182:489–496
18. Zidan F, Pajonk G, Germain E, Teichner SJ (1978) Kinetic studies and mechanism of the reaction of propylene nitric oxide for acrylonitrile synthesis in the presence of nickel oxide on alumina catalysts. J Catal 52:133–143
19. Menon PG (1979) On the mechanism of ammoxidation of propylene to acrylonitrile. J Catal 59:314–316
20. Germian JE, Pajonk G, Teichner SJ (1979) Comments on the mechanism of ammoxidation of propylene to acrylonitrile. J Catal 59:317–318
21. Meunier FC, Breen JP, Zuzaniuk V, Olsson M, Ross JRH (1999) Mechanistic aspects of the selective reduction of NO by propene over alumina and silver–alumina catalysts. J Catal 187:493–505
22. Breen JP, Burch R, Fontaine-Gautrelet C, Hardacre C, Rioche C (2008) Insight into the key aspects of the regeneration process in the NOx storage reduction (NSR) reaction probed using fast transient kinetics coupled with isotopically labelled 15NO over Pt and Rh-containing Ba/Al_2O_3 catalysts. Appl Catal B Environ 81:150–159
23. Chansai S, Burch R, Hardacre C, Naito S (2014) Origin of double dinitrogen release feature during fast switching between lean and rich cycles for NOx storage reduction catalysts. J Catal 317:91–98
24. Dasari P, Muncrief R, Harold MP (2013) Cyclic lean reduction of NO by CO in Excess H_2O on Pt–Rh/Ba/Al_2O_3: elucidating mechanistic features and catalyst performance. Top Catal 56:1922–1936
25. Bártova S, Kočí P, Mráček D, Marek M, Pihl JA, Choi JS, Toops TJ, Partridge WP (2013) New insights on N_2O formation pathways during lean/rich cycling of a commercial lean NOx trap catalyst. Catal Today 231:145–154
26. Mráček D, Kočí P, Marek M, Choi J-S, Pihl JA (2015) Dynamics of N_2 and N_2O peaks during and after the regeneration of lean NOx trap. Appl Catal B Environ 166–167:509–517
27. Zheng Y, Li M, Harold M, Luss D (2015) Enhanced low-temperature NOx conversion by high-frequency hydrocarbon pulsing on a dual layer LNT-SCR catalyst. SAE Int J Engines 8:2015-01-0984
28. Clayton RD, Harold MP, Balakotaiah V, Wan CZ (2009) Pt dispersion effects during NOx storage and reduction on Pt/BaO/Al_2O_3 catalysts. Appl Catal B Environ 90:662–676
29. Nguyen H, Harold MP, Luss D (2015) Spatiotemporal behavior of Pt/Rh/CeO_2/BaO catalyst during lean-rich cycling. Chem Eng Journal 262:464–477
30. NIST Chemistry WebBook https://webbook.nist.gov/chemistry
31. Kumar A, Zheng X, Harold MP, Balakotaiah V (2011) Microkinetic modeling of the NO+H_2 system on Pt/Al_2O_3 catalyst using temporal analysis of products. J Catal 279:12–26
32. Clayton RD, Harold MP, Balakotaiah V (2008) NOx storage and reduction with H2 on Pt/BaO/Al_2O_3 monolith: spatio-temporal resolution of product distribution. Appl Catal B Environ 84:616–630
33. Lietti L, Forzatti P, Nova I, Tronconi E (2001) NOx storage reduction over Pt–Ba/γ-Al_2O_3 catalyst. J Catal 204:175–191
34. Lesage T, Verrier C, Bazin P et al (2003) Studying the NO_x-trap mechanism over a Pt-Rh/Ba/Al_2O_3 catalyst by operando FT-IR spectroscopy. Phys Chem Chem Phys 5:4435–4440
35. Bisaiji Y, Yoshida K, Inoue M, Takagi N, Fukuma T (2012) Reaction mechanism analysis of Di-Air-contributions of hydrocarbons and intermediates. SAE Int J Fuels Lubr 5:1310–1316
36. Kumar A, Medhekar V, Harold MP, Balakotaiah V (2009) NO decomposition and reduction on Pt/Al_2O_3 powder and monolith catalysts using the TAP reactor. Appl Catal B Environ 90:642–651